HHS Public Access

Author manuscript

J Invest Dermatol. Author manuscript; available in PMC 2024 November 01.

Published in final edited form as:

J Invest Dermatol. 2023 November ; 143(11): 2163–2176.e6. doi:10.1016/j.jid.2023.04.031.

Merkel cell polyomavirus T-antigen-mediated reprogramming in adult Merkel cell progenitors

Madison Weber[1], **Minh Binh Nguyen**[1], **Meng Yen Li**[1], **Pooja Flora**[1], **Masahiro Shuda**[2], **Elena Ezhkova**[1]

[1]Black Family Stem Cell Institute, Department of Cell, Developmental, and Regenerative Biology, Icahn School of Medicine at Mount Sinai, New York, NY 10029, USA.

[2]Cancer Virology Program, Hillman Cancer Center, University of Pittsburgh, Pittsburgh, PA 15213, USA.

Abstract

Whether Merkel cells regenerate in adult skin and from which progenitor cells is a subject of debate. Understanding Merkel cell regeneration is of interest to the study of Merkel cell carcinoma (MCC), a rare neuroendocrine skin cancer hypothesized to originate in a Merkel cell progenitor transformed by Merkel cell polyomavirus (MCV) small (sT-Ag) and large (LT-Ag) T-antigens. We sought to understand what the adult Merkel cell progenitors are and whether they can give rise to MCC. We utilized lineage tracing to identify SOX9-expressing (SOX9+) cells as Merkel cell progenitors in postnatal murine skin. Merkel cell regeneration from SOX9+ progenitors occurs rarely in mature skin unless in response to minor mechanical injury. MCV sT-Ag and functional imitation of LT-Ag in SOX9+ cells enforced neuroendocrine and Merkel cell lineage reprogramming in a subset of cells. These results identify SOX9+ cells as postnatal Merkel cell progenitors that can be reprogrammed by MCV T-antigens to express neuroendocrine markers.

INTRODUCTION

Skin is a complex organ with a diverse array of functions which include providing a barrier against environmental insults, regulating body temperature, and detecting sensory information (Abdo et al., 2020). These activities are enabled by sub-structures within the skin, such as the epidermis and hair follicles, and specialized cells like Merkel cells. Merkel cells are neuroendocrine cells that provide tactile sensory information through

Correspondence and requests for materials should be addressed to E.E., elena.ezhkova@mssm.edu, 212-241-7184, Mt Sinai School of Medicine, One Gustave L. Levy Place, Box 1020, New York, NY 10029-6574, Twitter: @EzhkovaLab.
These authors contributed equally: Madison Weber, Minh Binh Nguyen, Meng Yen Li

AUTHOR CONTRIBUTIONS

Conceptualization: M.W., M.B.N., M.Y.L., P.F., and E.E.; Investigation and Visualization: M.W., M.B.N., M.Y.L.; Methodology: M.W., M.B.N., M.Y.L., P.F., M.S., and E.E.; Formal Analysis: M.W. and M.B.N.; Funding Acquisition: E.E.; Writing – Original Draft Preparation: M.W.; Writing – Review and Editing: M.W., M.B.N., M.Y.L., P.F., M.S., and E.E.

CONFLICT OF INTEREST STATEMENT

The authors declare no competing interests.

their innervation by afferent sensory neurons (Haeberle and Lumpkin, 2008; Owens and Lumpkin, 2014; Woo et al., 2015). Merkel cells are also the namesake of a rare neuroendocrine skin cancer, Merkel cell carcinoma (MCC) (Tang and Toker, 1979). Although it is rare, a MCC diagnosis is often lethal, and its incidence is increasing worldwide (Paulson et al., 2018).

Almost all MCC tumors contain DNA from Merkel cell polyomavirus (MCV), which is integrated clonally in every cell of a MCC tumor (Feng et al., 2008; Stakaityte et al., 2014; Tolstov et al., 2009). From this observation, it is inferred that MCC arises from a single MCV+ origin cell which clonally expands to generate the tumor. This expansion is driven by viral small T-antigen (sT-Ag) and Large T-antigen (LT-Ag) (Feng et al., 2008; Kervarrec et al., 2019a; Stakaityte et al., 2014), which MCC cell lines are dependent on for continued growth (Hesbacher et al., 2016; Houben et al., 2012). MCV sT-Ag enacts transcriptional change to incite histone remodeling, repress differentiation, inhibit tumor suppressor activity, and promote neuroendocrine transcription factor activation (Cheng et al., 2017; Leiendecker et al., 2020; Park et al., 2020; Sheng et al., 2018; Sihto et al., 2011). MCV LT-Ag deregulates the cell cycle by sequestering retinoblastoma (Rb1) protein (Hesbacher et al., 2016). Virus-positive MCC tumors demonstrate few mutations apart from MCV integration (Knepper et al., 2019), implicating sT-Ag and LT-Ag as the primary drivers of MCC tumorigenesis. However, much of the process by which the T-antigens initiate a MCC tumor is unclear, including and, in part, *because* we lack knowledge of the MCC cell of origin.

It was previously thought that MCC arose from Merkel cells because MCC expresses several markers which are otherwise unique in skin to Merkel cells (Tilling and Moll, 2012). However, attempts to generate MCC in mice by expressing T-antigens in Merkel cells demonstrated that Merkel cells are not responsive to oncogenic stimulation, leaving it unclear where MCC emerges from (Shuda et al., 2015). There is mounting evidence that MCC may originate within the epidermis or its appendages: the hair follicles. MCC expresses epidermal stem cell markers LGR5, LRIG1, and SOX9 (Sundqvist et al., 2021), and case studies have identified MCC tumors sharing ancestry with nearby tumors known to derive from the epidermis (Iacocca et al., 1998; Kervarrec et al., 2020a; Kervarrec, 2021). Furthermore, human scalp hair follicles develop Merkel cell-like clusters in response to MCV T-antigen expression (Kervarrec et al., 2020b), which may imply the ability of this population to give rise to MCC. However, expressing T-antigens in cytokeratin 5 (KRT5)-expressing (KRT5+) epidermis or KRT14+ keratinocytes in mice causes phenotypes resembling squamous or basal cell carcinomas, not MCC (Spurgeon et al., 2015; Verhaegen et al., 2017; Verhaegen et al., 2015).

Transcription factor Atonal homolog 1 (ATOH1) is the master regulator of Merkel cell fate (Perdigoto et al., 2014). Overexpressing ATOH1 in epidermis reprograms epidermal cells to the Merkel cell lineage, resulting in the formation of ectopic Merkel cells (Ostrowski et al., 2015). Based on the idea that MCC could be related to Merkel cells, Verhaegen et al. reported transgenic mouse models wherein epidermal cells were induced to overexpress ATOH1 in conjunction with MCV T-antigens. Targeting these epidermal cells, now reprogrammed to a Merkel cell fate, with T-antigens resulted in MCC-like

cell phenotypes (Verhaegen et al., 2022; Verhaegen et al., 2017). These results imply that commitment to the Merkel cell lineage is a key feature of the MCC cell of origin and that a Merkel cell progenitor would be an interesting candidate. However, whether a Merkel cell progenitor population exists in adult skin is not determined.

Most insights into Merkel cell biology come from studies using murine back skin. During development, Merkel cells derive from the KRT14-expressing basal keratinocyte layer (Van Keymeulen et al., 2009; Morrison et al., 2009; Woo et al., 2010) and are further specified from a series of progenitor populations localized to the developing hair follicle marked by KRT17 and SOX9 (Jenkins et al., 2019; Nguyen et al., 2018). Whether Merkel cells regenerate in adult skin and if any of these populations still act as Merkel cell progenitors postnatally is a subject of debate. One batch of evidence argues that the Merkel cell population established *in utero* is long-lived and does not undergo turnover postnatally (Wright et al., 2017; Wright et al., 2015). Other studies report that Merkel cells regenerate from epidermal populations on an ongoing basis (Doucet et al., 2013; Van Keymeulen et al., 2009; Xiao et al., 2015). Even between studies reporting Merkel cell regeneration in adult skin, there is not consensus about the timing (Marshall et al., 2016). Thus, the available data are not an adequate picture of Merkel cell regeneration at homeostasis.

Our laboratory previously discovered that SOX9-expressing (SOX9+) epidermal cells are embryonic Merkel cell progenitors (Nguyen et al., 2018). This led us to ask whether SOX9+ cells also give rise to Merkel cells in postnatal skin and if this population can be reprogrammed toward the neuroendocrine lineage by MCV T-antigens as is observed in MCC. To address both questions, we generated transgenic mouse models which selectively target SOX9+ cells for lineage tracing or for reprogramming by MCV T-antigens. We show that SOX9+ cells not only give rise to Merkel cells postnatally but can also be reprogrammed by MCV T-antigens to express neuroendocrine markers and form hyperproliferative lesions. Our results offer insights into Merkel cell biology and implicate SOX9+ Merkel cell progenitors as a potential origin of MCC.

RESULTS

SOX9+ cells are Merkel cell progenitors in postnatal skin.

To evaluate whether SOX9+ cells regenerate Merkel cells in postnatal skin, we performed lineage tracing experiments using $Sox9^{CreER};ROSA^{mT/mG}$ mice generated by crossing *C57BL/6-Sox9*$^{em1(cre/ERT2)Tchn/J}$ ($Sox9^{CreER}$) mice with *Gt(ROSA)26Sor*$^{tm4(ACTB-tdTomato,-EGFP)Luo/J}$ ($ROSA^{mT/mG}$) mice.

$Sox9^{CreER};ROSA^{mT/mG}$ mice were treated daily with tamoxifen injections from postnatal day (P) 22 until P24, and back skins were collected for immunofluorescence analysis at intervals thereafter (Figure 1a). The SOX9+ population in adult murine skin is mostly localized to the hair follicle (Nguyen et al., 2018). At P25, hair follicle cells were robustly labeled with GFP, indicating successful and specific Cre-mediated recombination (Figure 1b). Merkel cells do not express SOX9 (Figure S1a–c); accordingly, Merkel cells were largely not GFP+ at P25 (Figure 1b). 5 days after labeling, at P29, approximately 14.5% of KRT8+ Merkel cells were GFP+ (Figure 1c, f), indicating that new Merkel cells were

specified from the GFP-labeled SOX9+ population between P25 and P29. At P52, 16% of Merkel cells were GFP+ (Figure 1d, f).

To rule out the possibility that Merkel cells are self-renewing between P25 and P29, we performed EdU analysis at P21, P25, and P28. Although hair follicle cells showed EdU incorporation at P25 and P28, Merkel cells had not undergone division (Figure S2a–c). We also performed whole-mount staining for KRT8 (Figure S2d–g) to evaluate the relationship between regeneration and hair cycle. In mice, the first hair cycle is synchronized throughout the back skin with growth phase (anagen) from P28-P42, regression (catagen) from P42-P49, and resting phase (telogen) beginning at P49 (Schneider et al., 2009). We did not observe significant fluctuation in the number of Merkel cells corresponding to the stages of the hair cycle (Figure S2h), which implies that new Merkel cells arise to replace older ones rather than to expand the total Merkel cell population.

Taken together, these results demonstrate postnatal regeneration of Merkel cells from SOX9+ progenitor cells. This turnover does not occur rapidly or at a high frequency; rather, Merkel cells in adult skin are mostly long-lived.

SOX9+ progenitors retain Merkel cell regeneration potential in adulthood.

The increase in GFP+ Merkel cells between P52 and P150 was surprisingly small and not significant (Figure 1f). To clarify this observation, we induced GFP labeling in $Sox9^{CreER};ROSA^{mT/mG}$ mice at P50-P52 (Figure 2a). At P150, no Merkel cells were GFP+ (Figure 2b), while GFP+ cells were present in hair follicles. This observation indicates that Merkel cells regenerate only rarely in adult skin.

Wright et al. observed that new Merkel cells were produced in adult skin subjected to superficial injury (Wright et al., 2017). To examine whether SOX9+ cells could be stimulated to regenerate Merkel cells in adult skin, we induced GFP labeling in $Sox9^{CreER};ROSA^{mT/mG}$ mice at P50-P52 and subjected the back skins to waxing or repeated shaving. Back skins were collected after the fifth shave (Figure 2c) or one complete hair cycle after waxing (Figure 2g). Unperturbed skin sections from the same animals were collected as controls.

Consistent with previous observations, un-shaved control skin did not regenerate Merkel cells (<2%, Figure 2d, e). In contrast, approximately 10% of Merkel cells were GFP+ in shaved skin (Figure 2d, f). Similar observations were made in waxed animals, where <4.5% of Merkel cells regenerated in un-waxed skin (Figure 2h, i), but 14.5% of Merkel cells were GFP+ after waxing (Figure 2h, j). That is, SOX9+ cells resumed Merkel cell regeneration specifically in skin subjected to shaving or waxing, but not in adjacent unbothered skin. These observations show that SOX9+ cells remain a reservoir of Merkel cell progenitors in adult skin. Even though they do not regenerate Merkel cells frequently at homeostasis, these cells retain the potential to undergo Merkel cell differentiation and can be reactivated as Merkel cell progenitors.

MCV sT-Ag generates cutaneous lesions from SOX9+ cells.

Considering that MCC expresses SOX9 (Sundqvist et al., 2021) and our observation that SOX9+ cells can undergo Merkel cell differentiation, we wondered if SOX9+ Merkel cell progenitors could be reprogrammed by MCV T-antigens to express neuroendocrine and MCC markers. To probe this question, we first crossed *Rosa26-flox-stop-flox-sT-Ag* (*ROSA*$^{sT/sT}$) mice to *Sox9*^{CreER} mice to generate *Sox9*^{CreER};*ROSA*$^{sT/+}$ (sT) mice. Six months after topical 4-hydroxytamoxifen (4OHT) treatment (Figure 3a), the dorsal skin of sT mice developed small cutaneous lesions apparent in hematoxylin and eosin (H&E) staining as dermally located, spherical cell clusters with follicular histology (Figure 3b). Western blot confirmed the expression of sT-Ag in the lesions (Figure 3c). About half of all tumors appearing in the skin contained cells that expressed KRT8 (Figure 3d). The other half of the lesions in sT skin were morphologically similar but did not have widespread KRT8 expression; these tumors were not considered for further analysis. KRT8 is a marker typically expressed most robustly in skin by Merkel cells (Moll et al., 1995); however, unlike Merkel cells, which are terminally differentiated and mitotically inactive (Shuda et al., 2015), a number of KRT8+ tumor cells were proliferative (Figure 3d).

sT tumors did not express Merkel cell markers other than KRT8, including insulin gene-enhancer protein 1 (ISL1; Figure 3e) or special AT-rich sequence-binding protein 2 (SATB2; Figure 3f) (Fukuhara et al., 2016; Kervarrec et al., 2019b; Perdigoto et al., 2014). Tumors in sT mice also did not express neuroendocrine markers often expressed in MCC (Fujino et al., 2015; Gu et al., 1983; Leblebici et al., 2019; Rush et al., 2018) such as insulinoma-associated 1 (INSM1; Figure 3g) or neuron-specific enolase (NSE; Figure 3h), which is also expressed in some Merkel cells (Nguyen et al., 2019). Therefore, although sT-Ag expression can produce tumors from SOX9+ cells, it is not sufficient to instigate neuroendocrine differentiation or induce expression of MCC markers other than KRT8.

Rb1 loss is not tumorigenic in SOX9+ cells.

Rb1 inhibition is the principal contribution of MCV LT antigen to MCC tumorigenesis (Hesbacher et al., 2016; Houben et al., 2012). By sequestering Rb1, LT-Ag deregulates the cell cycle (Richards et al., 2015) and promotes reprogramming (Kareta et al., 2015). Functionally separating sT-Ag and LT-Ag is challenging because they are co-expressed as splice variants (Feng et al., 2008); therefore, to test the ability of LT-Ag alone to reprogram SOX9+ cells, we generated and treated *Sox9*^{CreER};*Rb*$^{flox/flox}$ (Rb^{KO}) mice (Figure S3a). 6 months after treatment, effective knockdown of Rb1 in hair follicle (Figure S3c) resulted in no appreciable changes to the phenotype of the skin (Figure S3b). Rb^{KO} mice did not develop hyperproliferation in hair follicles (Figure S3d), nor aberrantly express Merkel cell lineage or neuroendocrine markers (Figure S3e–h). Therefore, we concluded that Rb1 inhibition alone is not tumorigenic in and does not reprogram SOX9+ cells.

sT-Ag and Rb1 loss promote neuroendocrine reprogramming of SOX9-derived tumors.

To test whether inhibiting Rb1 in tandem with sT-Ag expression could instigate neuroendocrine reprogramming in SOX9+ cells, we generated *SOX9*^{CreER};*ROSA*$^{sT/+}$;*Rb*$^{flox/flox}$ (sT+Rb^{KO}) mice. Six months following topical 4OHT treatment, sT+Rb^{KO} mice developed lesions in the back skin (Figure 4a) with similar

histology to the sT tumors (Figure 4b). The size of sT+Rb^{KO} tumors varied considerably, as did the number of tumors in each animal, but there was no obvious trend with sex or between littermates. Western blot and IF confirmed expression of sT-Ag in sT+Rb^{KO} tumors (Figure 4c) and loss of Rb1 in tumors and hair follicles of sT+Rb^{KO} mice (Figure 4d).

Roughly two-thirds of all the tumors appearing in sT+Rb^{KO} mice expressed KRT8. Like in sT animals, some smaller growths were negative for KRT8; these were not considered for further analysis. Many KRT8+ tumor cells were proliferative (Figure 4e). IF and Western blot revealed that many KRT8+ sT+Rb^{KO} tumor cells also expressed Merkel cell markers ISL1, SATB2, and KRT20 (Figure 4f, g, j) as well as neuroendocrine markers INSM1, NSE, and chromogranin A (CHGA) (Figure 4h, i, j). The expression of these markers was not uniform: not all KRT8+ tumors expressed other Merkel cell or neuroendocrine markers, and not all KRT8+ cells within a tumor also expressed another neuroendocrine marker. Table 1 presents the average proportion of DAPI cells expressing each marker, as well as the proportion of cells which were co-positive for KRT8 and another marker.

The expression of neuroendocrine differentiation markers in SOX9-derived tumors illustrates that the SOX9+ population is permissive to reprogramming mediated by sT-Ag expression and Rb1 ablation to mimic LT-Ag.

KRT8+ tumors do not express hallmarks of basal or squamous cell carcinoma.

Consistent with their origin within the hair follicle, sT and sT+Rb^{KO} tumors expressed epidermal cytokeratins KRT5, KRT14, KRT17, and KRT15 (Figure S4a–d), indicating that sT-Ag expression and Rb1 ablation did not cause a complete departure from the hair follicle identity of SOX9+ cells. Since the epidermis and hair follicle are established origins for basal cell and squamous cell carcinomas (BCC and SCC) (Peterson et al., 2015), we investigated the expression of archetypal BCC and SCC markers in sT and sT+Rb^{KO} tumors. None of the SOX9-derived lesions expressed BCC/hair follicle stem cell marker CD34 (Figure S5a) (Díaz-Flores et al., 2021; Sur et al., 2007), epidermal keratinocyte marker KRT10 (Figure S5b), which can be associated either BCC or SCC (Uhlig et al., 2022), or SCC-specific marker PITX1 (Figure S5c) (LiboRio et al., 2011). Therefore, we conclude that tumors expressing markers of neuroendocrine differentiation are not variants of BCC or SCC, which is consistent with patient data reporting that MCV T-antigens are not detected in cutaneous tumors other than MCC (Dworkin et al., 2009).

SOX9-derived tumors acquire neuroendocrine markers over time.

To examine how SOX9+ cell reprogramming occurs, we collected the back skins of sT+Rb^{KO} mice at earlier time points 2- and 4-months after treatment (at P110 and P170) (Figure 5a). As SOX9+ cells are mostly located in the hair follicles (Figure 1 and Figure S1), we focused on the changes induced in these skin appendages. 2 months post-treatment at P110, the hair follicles of sT+Rb^{KO} mice had appreciably expanded and penetrated deeply into the dermis (H&E, Figure 5b). Several of the hair follicles undergoing expansion, indicated by proliferation marker Ki67, also expressed KRT8 at P110, 2 months post-treatment (Figure 5c). Ultimately, the upper portion of the hair follicles collapsed, resulting in KRT8+ lesions with no epidermal attachments forming between 4- and 6-months post-

treatment (P170-P230). The disappearance of the upper hair follicle may have occurred through cell death: cleaved caspase 3 IF and TUNEL assay indicated high numbers of apoptotic/dying cells in hair follicles 2 months post-treatment at P110, but cell death was comparably low in the skins of sT+RB^{KO} mice at P170 and P230 (Figure 5d, Figure S6a).

Neither KRT8+ nor KRT8- cells expressed neuroendocrine markers at P110, 2 months after treatment (Figure 6a–d). Only P170 tumors 4 months post-treatment expressed neuroendocrine markers ISL1 (Figure 6a), SATB2 (Figure 6b), INSM1 (Figure 6c), or NSE (Figure 6d). These observations illustrate that neuroendocrine reprogramming progresses throughout the development of sT+Rb^{KO} tumors; meanwhile, cells that are only partially reprogrammed by sT-Ag expression and Rb1 ablation are eliminated. Critically, although the interfollicular epidermis was also hyperproliferative 2 months post-treatment at P110, the appearance of KRT8+ cells was restricted to the hair follicles.

Altogether, the results showed expression of Merkel cell and neuroendocrine markers in sT+Rb^{KO} lesions, but not differential diagnostic markers of other skin cancers, demonstrating that SOX9+ Merkel cell progenitor cells are susceptible to neuroendocrine reprogramming by MCV T- antigens.

DISCUSSION

Our research consolidates experimental approaches from across the literature to present a unified examination of postnatal Merkel cell regeneration. Merkel cells originate from SOX9+ progenitors during development (Nguyen et al., 2018); our findings show that this population retains the ability to regenerate Merkel cells after birth. At homeostasis, Merkel cell specification from SOX9+ progenitors occurs prior to P29, but Merkel cell turnover becomes rare when the skin reaches maturity. This is consistent with observations that more Merkel cells form within the four weeks after birth than afterward (Doucet et al., 2013; Woo et al., 2010) and prompts interesting questions about why and how such a switch occurs. It could be tied to postnatal development: mice undergo substantial growth in the weeks after birth, which includes growing their first coat of hair. The SOX9-derived Merkel cell specification before P29 may therefore be morphogenic rather than regenerative. However, SOX9+ cells remain capable of acting as Merkel cell progenitors and can be stimulated to regenerate Merkel cells by insult to the epidermis.

Merkel cell numbers decrease with advanced age in both mice and humans (Feng et al., 2018; García-Piqueras et al., 2019) along with the ability to sense fine texture (Skedung et al., 2018), perhaps because more Merkel cells die than are replaced in aged skin. Loss of Merkel cells may also have a causal relationship with chronic itch (Feng et al., 2018). Our experiments demonstrating Merkel cell regeneration in waxed and shaved skin hint at a potential link between Merkel cell regeneration to the pathogenesis of psoriasis as well: psoriatic skin has increased Merkel cells compared to healthy skin (Wollina and Mahrle, 1992), and new lesions often form at the site of minor injuries like shaving and waxing (Martin et al., 2021). Understanding the mechanisms of Merkel cell maintenance could be leveraged to treat these and other conditions by bolstering or ablating normal regeneration processes.

The SOX9+ hair follicle population is conserved in humans (Shi et al., 2013). We propose a model of MCC initiation wherein viral T-antigens expressed upon MCV integration promote Merkel cell-like differentiation and clonal expansion from Merkel cell progenitors. This model would be consistent with our previous report showing that MCV T-antigens promote the expression of Merkel cell markers in MCV+ MCC cells *in vitro* (Harold et al., 2019).

Human scalp hair follicles transduced with MCV T-antigens develop neuroendocrine cell clusters, which illustrates this population's ability to be reprogrammed by MCV in humans in a manner similar to what we observed in sT+Rb^{KO} mice (Kervarrec et al., 2020b). Moreover, a recent study in mice found that even when MCV T-antigens are expressed in nearly all cells in the epidermis, nascent neuroendocrine tumor cells arise specifically within the hair follicle (Verhaegen et al., 2022). Consistent with these observations, we observe that MCV sT-Ag expression combined with Rb1 ablation reprograms SOX9+ hair follicle cells to expand and form lesions that express neuroendocrine and Merkel cell markers. Our results highlight the SOX9+ population as an interesting candidate for further study in pursuit of the MCC cell of origin.

By substituting Rb1 knockout for LT-Ag expression, we were able to functionally isolate LT-Ag and sT-Ag. This is otherwise challenging because they are co-expressed as splice variants of the same region (Feng et al., 2008). We found that sT-Ag is required for tumorigenesis, since sT-Ag independently drove hyperproliferation, whereas Rb1 loss alone did not cause tumorigenesis. Meanwhile, expression of neuroendocrine and Merkel cell markers in SOX9-derived, sT-Ag driven tumors was contingent upon ablation of Rb1. In addition to repressing Rb1's cell cycle regulatory functions, LT-Ag-mediated interaction with Rb family proteins is responsible for the upregulation of certain Merkel cell lineage genes in MCC (Harold et al., 2019). Functional Rb1 represses pluripotency networks to maintain differentiation states (Giacinti and Giordano, 2006; Kareta et al., 2015), so Rb1 suppression may create a permissive cell state for sT-Ag to enact neuroendocrine reprogramming. Conversely, functional Rb1 protein restricts the genes sT-Ag can engage with and therefore limits the scope of sT-Ag-driven reprogramming. Thus, the result that both sT-Ag expression and Rb1 knockout were required to generate lesions expressing Merkel cell and neuroendocrine markers.

Our results highlight the SOX9+ population as having potential links to the MCC cell of origin. Many of the markers we observed in sT+Rb^{KO} lesions are characteristic of MCC but not present in the epidermis nor in other cutaneous tumors known to derive from the epidermis. Importantly, this includes INSM1, KRT20, and CHGA, which are closely associated with MCC and are used as differential diagnostic markers of the disease in cases that resemble other cutaneous tumors (Coggshall et al., 2018; Paulson et al., 2018). At the same time, the reprogramming in sT+Rb^{KO} tumors did not terminate the hair follicle lineage, which is inconsistent with human MCCs. We have several ideas why that might have occurred and how future work might overcome this hurdle.

First, it is possible that Rb1 knockout did not completely mimic LT-Ag. MCV LT-Ag is a viral replicase that binds viral DNA and initiates replication (Shuda et al., 2008). In MCC, LT-Ag undergoes a truncation event upon integration which eliminates its C-terminal DNA

binding and helicase domains(Feng et al., 2008; Shuda et al., 2008). The remaining form of MCV LT-Ag contains a DnaJ domain, which interacts with heat shock proteins (Shuda et al., 2008), and a pocket protein-binding (LxCxE) motif that interacts with Rb1 and other Rb family members Rb2/p130 and Rb3/p107 (Feng et al., 2008). Outside of these domains, truncated LT-Ag also interacts with Vam6p (Liu et al., 2011) and BRD4 (Arora et al., 2019; Wang et al., 2012). Rb1 suppression is the essential function of LT-Ag through which it enacts most of its effects in MCC tumors (Harold et al., 2019; Houben et al., 2012; Liu et al., 2011; Richards et al., 2015), hence our substitution of LT-Ag with Rb1 knockout. However, it is possible that any of these other LT-Ag interactions play roles in MCC which are not recapitulated by Rb1 knockdown.

We observed a substantial lack of uniformity between reprogrammed cells in sT+Rb^{KO} mice, including a subset of lesions in sT+Rb^{KO} mice that lacked appreciable expression for any of the neuroendocrine markers. This is potentially due to the heterogeneity of the SOX9+ population. We speculate that the cells that underwent expansion but never expressed neuroendocrine markers originated in SOX9+ subpopulations which are resistant to reprogramming. This hypothesis implies that only specific subpopulations within the SOX9+ cells can be reprogrammed by the T-antigens, which is consistent with our observation that only some cells expressed KRT8 at the early stages of reprogramming in sT+Rb^{KO} skin. Further experimentation in this avenue should seek to identify likely Merkel cell progenitor subpopulations and test the re-programmability of them.

Finally, our observation that neuroendocrine markers are expressed only 6 months after induction sT expression and Rb1 ablation in SOX9+ cells raises the question of whether the reprogramming process can be accelerated. It is unclear what factor limits the expansion and reprogramming of SOX9+ cells, but our observation of apoptosis in sT+Rb^{KO} skin at earlier stages of reprogramming leads us to think that p53 activity may be involved. p53 suppression has received attention as a factor in MCC tumorigenesis which contributes substantially to both tumor initiation and sustained growth (Park et al., 2019; Shuda et al., 2015; Verhaegen et al., 2022). Our model does not manipulate p53 directly, and to explore p53 transcription status or activity in the reprogrammed SOX9+ cells was outside the scope of our current study. However, future explorations into murine models should consider including p53 ablation alongside and instead of MCV T-antigens to elaborate on its contribution to MCC tumorigenesis and potentially promote more advanced reprogramming.

MATERIALS AND METHODS

Mice

Mice were housed at the Icahn School of Medicine at Mount Sinai Center for Comparative Medicine and Surgery (CCMS). Animal protocols used for this study were approved by the Association for Assessment and Accreditation of Laboratory Care International (AAALACi)-accredited Icahn School of Medicine at Mount Sinai Institutional Animal Care and Use Committee (IACUC) (IPROTO202100000011). *C57BL/6-Sox9$^{em1(cre/ERT2)Tchn/J}$* (*$Sox9^{CreER}$*) was described (Xu et al., 2015). *STOCK $Rb1^{tm2Brn}$* (*$Rb^{flox/flox}$*) (Stock number: 026563) and *B6.129(Cg)-Gt(ROSA)26Sor$^{tm4(ACTB-tdTomato,-EGFP)Luo}$* (*$ROSA^{mT/mG}$*) (Stock number: 007676) mice were obtained from The Jackson Laboratory. *$ROSA^{sT/sT}$* mice were

provided by Patrick Moore (University of Pittsburgh; Pittsburgh, PA). Mice were genotyped by PCR using DNA extracted from toes. Genotyping primers are below.

Treatments

Sox9-CreER;*R26-mT/mG* mice were injected interperitoneally daily for 3 consecutive days with 100 μg/g body weight Tamoxifen (Sigma-Aldrich; St. Louis, MO) dissolved in corn oil. Waxing or the first shaving of mice was performed 3 days after the final injection. *Sox9-CreER;sT-Ag*, *Sox9-CreER;Rb*$^{flox/flox}$, and *Sox9-CreER;sT-Ag+Rb*$^{flox/flox}$ mice were treated topically daily for 4 consecutive days beginning at P50 with 4-hydroxy-tamoxifen (Sigma-Aldrich; St. Louis, MO) dissolved in 100% ethanol. Mouse back fur was clipped short with an animal hair trimmer so that 100 μL of 2mg/mL (20 μg) 4OHT ethanol solution could be pipetted directly on skin. For all animals, euthanasia was performed using carbon dioxide and tissues were collected immediately. At least 3 animals from separate litters were used for each analysis.

EdU injection

Wild-type C57BL/6 mice were injected with 10 μg/g body weight EdU solution (Salic and Mitchison, 2008). Skin was collected 24h after injection and embedded fresh in OCT. Slides were cut into sections using a Leica Cryostat and stored at −80°C until use. Slides were fixed in 4% paraformaldehyde and permeabilized in 0.5% Triton, followed by washes with 3% BSA and 30 minutes incubation in Click-iT reaction cocktail (ThermoFisher, C10337). Slides were washed twice more before proceeding to immunofluorescence blocking and staining.

Immunofluorescence

Tissue was collected from mice and embedded fresh into OCT without fixation. Slides were cut into 10 μm sections using a Leica Cryostat and stored at −80°C until use. Slides were fixed for 10 minutes in 4% PFA, then blocked for 1 hour at room temperature in a blocking solution containing 0.1% Triton X-100, 1% bovine serum albumin, and 0.5% normal donkey serum. Primary antibodies were diluted in blocking solution and incubated overnight at 4°C, followed by incubation in Alexa Fluor secondary antibodies (1:500 in blocking solution) for 1–2 hours at room temperature. Slides were counterstained with DAPI and mounted using propyl-gallate anti-fade mounting media. For Rb1 immunofluorescence, primary antibody was incubated for 1 hour at room temperature and subjected to additional washes after primary and secondary antibody. For SATB2 immunofluorescence, skin sections were permeabilized for 10 minutes in 0.5% Triton X-100 prior to blocking. For slides stained with mouse antibodies, Mouse-On-Mouse Immunodetection Kit (VECTOR labs) reagents were added to blocking solution according to manufacturer's recommendations.

For whole-mount immunofluorescence, back skins were collected and fixed in 4% PFA for 3 hours. Skins were blocked overnight in blocking solution. Primary antibodies diluted in blocking solution were incubated for 48 hours at room temperature, followed by incubation in secondary antibodies for 24 hours at room temperature. Skins were counterstained with DAPI and mounted using anti-fade mounting media.

Western Blotting

Control skin and tumors excised from OCT blocks were lysed directly in 60 mM Tris-HCl (pH 6.8), 10% glycerol, 2% SDS buffer with 0.1% 2-mercaptoethanol. Lysate was denatured by boiling for 10 minutes at ≥95°C immediately prior to loading in a 10% SDS-PAGE gel. After transfer, membranes were blocked 30 minutes in 5% bovine serum albumin blocking solution prepared in PBST (1x PBS supplemented with 0.2% Tween-20). Primary antibody was diluted in blocking solution and incubated overnight at 4°C; secondary HRP conjugate antibodies (VECTOR labs) diluted in PBST were incubated 1 hour at room temperature. Antigen detection was performed with Lumi-Light Western Blotting Substrate (Roche, 12015200001) according to manufacturer's instructions.

Microscopy and Quantification

Slides were imaged using a Leica DM5500 upright microscope or Confocal Zeiss LSM880 Airyscan microscope. Quantification of Merkel cells per touch dome was performed by manually counting all positively stained and co-stained cells from each section examined. The mean proportion of co-stained cells for each animal was calculated and used in statistical analysis. Quantification of cells in sT+Rb^{KO} lesions was performed by manually counting cells from each section examined. Counts from all lesions were averaged to calculate the mean proportion of stained and co-stained cells.

Antibodies

Antibodies and dilutions were used as follows: Caspase 3 1:250 (R&D; 84390); CD34 1:100 (ThermoFisher; 14-0341-82); CHGA 1:500 IF, 1:100 WB (Abcam; ab15160); ECAD 1:500 (ThermoFisher; 13-1900); GFP 1:500 (Abcam; ab13970); H3 1:10,000 (Cell Signaling; 9733S); INSM1 1:500 IF, 1:1000 WB (SantaCruz; sc-271408); ISL1 1:250 (Abcam; ab86472); KRT5 1:500 (Biolegend; 905901); KRT8 1:250 IF and whole mount (DSHB; TROMA-1); KRT10 1:500 (Biolegend; 905401); KRT14 1:500 (Biolegend; 906001); KRT15 1:500 (Biolegend; 833901); KRT17 1:500 (Abcam; ab109725); KRT20 1:500 WB (Aligent; M701901–2); Ki67 1:500 (Abcam; ab15580); MCV sT-Ag 1:20 WB (CM5E1 (Shuda et al., 2011), provided by Dr. Patrick Moore, University of Pittsburgh); NSE 1:250 IF, 1:10,000 WB (Novus; NPB100–1606); PITX1 1:500 (Novus, NBP1–88644); RB1 1:500 (Novus; NBP2–20127); SATB2 1:100 or 1:250 (Abcam; ab92446); SOX9 1:500 (Abcam; ab185966).

Secondary antibodies used at 1:500 for IF were 488 donkey anti-chicken (Jackson Immuno; 703-545-155), 488 donkey anti-rabbit (Jackson Immuno; 711-545-152), 594 donkey anti-rat (Jackson Immuno; 712-585-150), 647 donkey anti-rat (Jackson Immuno; 712-605-150), 647 donkey anti-rabbit (Jackson Immuno; 711-605-152). Secondary antibodies used for WB were 1:10,000 ImPRESS HRP IgG anti-rabbit (VECTOR labs; MP-7401-15), 1:10,000 ImPRESS HRP IgG anti-mouse (VECTOR labs; MP-7402-15), and 1:5,000 Peroxidase AffiniPure Donkey Anti-Chicken IgG (Jackson Immuno; 703-035-155).

TUNEL

TUNEL assay was performed using Roche *in Situ* Cell Death Detection Kit, Fluorescein (Sigma-Aldrich; 11684795910) according to manufacturer's instructions. Cryopreserved

tissue slides were fixed for 20 minutes in 4% PFA and washed 30 minutes in PBS, followed by permeabilization for 2 minutes on ice in a solution of 0.1% Triton X-100, 0.1% sodium citrate. Slides were incubated in TUNEL reaction mixture for 2 hours at room temperature, counter stained with DAPI, and imaged immediately. Negative and positive control slides were included in each staining. Negative control sections were incubated in label solution without terminal transferase. Positive control staining was performed using sections incubated 15 minutes with DNase enzyme from the Qiagen RNase-Free DNase Set (Cat. No. 79254) (50 μL or 135 Kunitz units of enzyme in 50mM Tris-HCL, pH 7.5, 1mg/mL BSA) prior to TUNEL reaction mixture incubation.

Statistics

Statistical calculations were performed using GraphPad Prism software. To determine the significance between two groups, the Mann-Whitney test was used. Tests were one-tailed for GFP+/KRT8+ cell counts (Figures 1 and 2) and two-tailed for Merkel cell per touch dome counts (Figure S2h). The number of biological replicates for each sample group is indicated in figure legends and as follows: postnatal lineage tracing (Fig. 1f) P25 *n=4*, P29 *n=6*, P52 *n=4*, P150 *n=4*; Merkel cells per touch dome (Fig. S2h) P27 *n=4*, P35 *n=4*, P41 *n=4*, P41 *n=4*; shaved and waxed mice (Fig. 2d, h) *n=3* shaved, *n=3* waxed. For all statistical tests, a $p \leq 0.05$ was accepted for significance. Significant *p*-values are provided in the figure legends.

Genotyping

Primers used to genotype mice were as follows:

SOX9-CreER	SOX9-CreER_WT F – (CTT CCATCCCGCAGACCCA) SOX9-CreER_Common R – (ACAAAGTCCAAACAGGCAGGGA) SOX9-CreER_Mut F – (CGGGCTCTACTTCATCGCATTC)
mT/mG	mTmG 1 – (CTCTGCTGCCTCCTGGCTTCT) mTmG 2 – (CGAGGCGGATCACAAGCAATA) mTmG 3 – (TCAATGGGCGGGGGTCGTT)
MCV sT Ag	4719(11053-11071(F)) – (TGGTTCACGCCTGTAATC) 4723(sTco_C-term.F.2) – (CCGACTATTGCTTGCTTCAC)
Rb flox	26379 (F) – (CTCATGGACTAGGTTAAGTTGTGG) 26380 (R) – (GCATTTAATTGTCCCCTAATCC)

Supplementary Material

Refer to Web version on PubMed Central for supplementary material.

ACKNOWLEDGEMENTS

For help, critical reagents, and experimental input, we are grateful to Sergei Ezhkov and Drs. Michael Rendl, Timothy Blenkinsop, and Andrew Ji. We would like to thank Dr. Patrick Moore for his generous gift of the *ROSA*$^{sT/sT}$ mice and Dr. Ting Chen (National Institute of Biological Sciences, Beijing, China) for providing *C57BL/6-Sox9*$^{em1(cre/ERT2)Tchn}$*/J* mice. We also thank the personnel of the Microscope and Animal Care Facilities at the Icahn School of Medicine at Mount Sinai.

M.W. was a trainee of the National Cancer Institute Training Program T32CA078207 while performing this research. M.Y. L. was supported by a Training Program in Stem Cell Biology fellowship from the New York

State Department of Health NYSTEM-C32561GG. Research reported in this publication was supported by the National Institute of Arthritis and Musculoskeletal and Skin Diseases under award numbers R01AR063724 and P30AR079200 (E.E.) and Department of Defense Rare Cancer Program W81XWH2110564 (E.E.).

DATA AVAILABILITY STATEMENT

No datasets were generated or analyzed during the current study.

REFERENCES

Abdo JM, Sopko NA, Milner SM. The applied anatomy of human skin: A model for regeneration. Wound Med. Elsevier GmbH; 2020; 28

Arora R, Vats A, Chimankar V. MCV Truncated Large T antigen interacts with BRD4 in tumors. Matters. Matters (Zur); 2019; 2019

Cheng J, Park DE, Berrios C, White EA, Arora R, Yoon R et al. Merkel cell polyomavirus recruits MYCL to the EP400 complex to promote oncogenesis. PLoS Pathog. Public Library of Science; 2017; 13

Coggshall K, Tello TL, North JP, Yu SS. Merkel cell carcinoma: An update and review: Pathogenesis, diagnosis, and staging. J. Am. Acad. Dermatol. Mosby Inc; 2018. p. 433–42

Díaz-Flores L, Gutiérrez R, García MP, González-Gómez M, Rodríguez-Rodriguez R, Hernández-León N et al. Cd34+ Stromal Cells/Telocytes in Normal and Pathological Skin. Int. J. Mol. Sci. Multidisciplinary Digital Publishing Institute; 2021; 22:7342

Doucet YS, Woo S-H, Ruiz ME, Owens DM. The Touch Dome Defines an Epidermal Niche Specialized for Mechanosensory Signaling. CellReports 2013; 3:1759–65

Dworkin AM, Tseng SY, Allain DC, Iwenofu OH, Peters SB, Toland AE. Merkel cell polyomavirus in cutaneous squamous cell carcinoma of immunocompetent individuals. J. Invest. Dermatol. J Invest Dermatol; 2009; 129:2868–74 [PubMed: 19554019]

Feng J, Luo J, Yang P, Du J, Kim BS, Hu H. Piezo2 channel–Merkel cell signaling modulates the conversion of touch to itch. Science (80-.). American Association for the Advancement of Science; 2018; 360:530–3

Feng H, Shuda M, Chang Y, Moore PS. Clonal integration of a polyomavirus in human Merkel cell carcinoma. Science (80-.). American Association for the Advancement of Science; 2008; 319:1096–100

Fujino K, Motooka Y, Hassan WA, Ali Abdalla MO, Sato Y, Kudoh S et al. Insulinoma-associated protein 1 is a crucial regulator of neuroendocrine differentiation in lung cancer. Am. J. Pathol. Elsevier Inc; 2015; 185:3164–77

Fukuhara M, Agnarsdóttir M, Edqvist PH, Coter A, Ponten F. SATB2 is expressed in Merkel cell carcinoma. Arch. Dermatol. Res. Springer Verlag; 2016; 308:449–54

García-Piqueras J, García-Mesa Y, Cárcaba L, Feito J, Torres-Parejo I, Martín-Biedma B et al. Ageing of the somatosensory system at the periphery: age- related changes in cutaneous mechanoreceptors. J. Anat. Wiley-Blackwell; 2019; 234:839

Giacinti C, Giordano A. RB and cell cycle progression. Oncogene 2006 2538. Nature Publishing Group; 2006; 25:5220–7

Gu J, Polak JM, Path M, Van Noorden S, E Pearse AG, Path F et al. lmmunostaining of Neuron-Specific Enolase as a Diagnostic Tool for Merkel Cell Tumors. Cancer 1983; 52:1039–43 [PubMed: 6349776]

Haeberle H, Lumpkin EA. Merkel Cells in Somatosensation. Chemosens. Percept. NIH Public Access; 2008; 1:110

Harold A, Amako Y, Hachisuka J, Bai Y, Li MY, Kubat L et al. Conversion of Sox2-dependent Merkel cell carcinoma to a differentiated neuron-like phenotype by T antigen inhibition. Proc. Natl. Acad. Sci. U. S. A. National Academy of Sciences; 2019; 116:20104–14

Hesbacher S, Pfitzer L, Wiedorfer K, Angermeyer S, Borst A, Haferkamp S et al. RB1 is the crucial target of the Merkel cell polyomavirus Large T antigen in Merkel cell carcinoma cells. Oncotarget. Impact Journals LLC; 2016; 7:32956–68

Houben R, Adam C, Baeurle A, Hesbacher S, Grimm J, Angermeyer S et al. An intact retinoblastoma protein-binding site in Merkel cell polyomavirus large T antigen is required for promoting growth of Merkel cell carcinoma cells. Int. J. Cancer. John Wiley & Sons, Ltd; 2012; 130:847–56

Iacocca MV, Abernethy JL, Stefanato CM, Allan AE, Bhawan J. Mixed Merkel cell carcinoma and squamous cell carcinoma of the skin. J. Am. Acad. Dermatol. Mosby; 1998; 39:882–7

Jenkins BA, Fontecilla NM, Lu CP, Fuchs E, Lumpkin EA. The cellular basis of mechanosensory Merkel-cell innervation during development. Elife. eLife Sciences Publications Ltd; 2019; 8

Kareta MS, Gorges LL, Hafeez S, Benayoun BA, Marro S, Zmoos AF et al. Inhibition of pluripotency networks by the Rb tumor suppressor restricts reprogramming and tumorigenesis. Cell Stem Cell. Cell Press; 2015; 16:39–50

Kervarrec T, Aljundi M, Appenzeller S, Samimi M, Maubec E, Cribier B et al. Polyomavirus-Positive Merkel Cell Carcinoma Derived from a Trichoblastoma Suggests an Epithelial Origin of this Merkel Cell Carcinoma. J. Invest. Dermatol 2020a; 140:976–85 [PubMed: 31759946]

Kervarrec T, Samimi M, Guyétant S, Sarma B, Chéret J, Blanchard E et al. Histogenesis of Merkel cell carcinoma: A comprehensive review. Front. Oncol. Frontiers Media S.A; 2019a.

Kervarrec T, Samimi M, Hesbacher S, Berthon P, Wobser M, Sallot A et al. Merkel cell polyomavirus T antigens induce merkel cell-like differentiation in GLI1-expressing epithelial cells. Cancers (Basel). MDPI AG; 2020b; 12

Kervarrec T, Tallet A, Miquelestorena-Standley E, Houben R, Schrama D, Gambichler T et al. Diagnostic accuracy of a panel of immunohistochemical and molecular markers to distinguish Merkel cell carcinoma from other neuroendocrine carcinomas. Mod. Pathol. Nature Publishing Group; 2019b; 32:499–510

Van Keymeulen A, Mascre G, Youseff KK, Harel I, Michaux C, De Geest N et al. Epidermal progenitors give rise to Merkel cells during embryonic development and adult homeostasis. J. Cell Biol. Rockefeller University Press; 2009; 187:91–100

Knepper TC, Montesion M, Russell JS, Sokol ES, Frampton GM, Miller VA et al. The genomic landscape of Merkel cell carcinom and clinicogenomic biomarkers of response to immune checkpoint inhibitor therapy. Clin. Cancer Res. American Association for Cancer Research Inc; 2019; 25:5961–71

Leblebici C, Yeni B, Savli TC, Aydın Ö, Güneş P, Cinel L et al. A new immunohistochemical marker, insulinoma-associated protein 1 (INSM1), for Merkel cell carcinoma: Evaluation of 24 cases. Ann. Diagn. Pathol. W.B. Saunders; 2019; 40:53–8

Leiendecker L, Jung PS, Krecioch I, Neumann T, Schleiffer A, Mechtler K et al. LSD 1 inhibition induces differentiation and cell death in Merkel cell carcinoma. EMBO Mol. Med. EMBO; 2020; 12:e12525

LiboRio TN, Acquafreda T, Matizonkas-Antonio LF, Silva-Valenzuela MG, Ferraz AR, Nunes FD. In situ hybridization detection of homeobox genes reveals distinct expression patterns in oral squamous cell carcinomas. Histopathology. Histopathology; 2011; 58:225–33 [PubMed: 21323949]

Liu X, Hein J, Richardson SCW, Basse PH, Toptan T, Moore PS et al. Merkel cell polyomavirus large T antigen disrupts lysosome clustering by translocating human Vam6p from the cytoplasm to the nucleus. J. Biol. Chem 2011; 286:17079–90 [PubMed: 21454559]

Marshall KL, Clary RC, Baba Y, Orlowsky RL, Gerling GJ, Lumpkin EA. Touch Receptors Undergo Rapid Remodeling in Healthy Skin. Cell Rep. Elsevier B.V; 2016; 17:1719–27

Martin AA, Padgett JK, Mayo KB. Koebner Phenomenon. Consultant. StatPearls Publishing; 2021; 51:409

Moll I, Kuhn C, Moll R. Cytokeratin 20 is a general marker of cutaneous Merkel cells while certain neuronal proteins are absent. J. Invest. Dermatol. Nature Publishing Group; 1995; 104:910–5

Morrison KM, Miesegaes GR, Lumpkin EA, Maricich SM. Mammalian Merkel cells are descended from the epidermal lineage. Dev. Biol. Academic Press Inc; 2009; 336:76–83

Nguyen MB, Cohen I, Kumar V, Xu Z, Bar C, Dauber-Decker KL et al. FGF signalling controls the specification of hair placode-derived SOX9 positive progenitors to Merkel cells. Nat. Commun. Nature Publishing Group; 2018; 9

Nguyen MB, Valdes VJ, Cohen I, Pothula V, Zhao D, Zheng D et al. Dissection of Merkel cell formation in hairy and glabrous skin reveals a common requirement for FGFR2-mediated signalling. Exp. Dermatol. Exp Dermatol; 2019; 28:374–82 [PubMed: 30758073]

Ostrowski SM, Wright MC, Bolock AM, Geng X, Maricich SM. Ectopic Atoh1 expression drives Merkel cell production in embryonic, postnatal and adult mouse epidermis. Dev. Company of Biologists Ltd; 2015; 142:2533–44

Owens DM, Lumpkin EA. Diversification and specialization of touch receptors in skin. Cold Spring Harb. Perspect. Med. Cold Spring Harb Perspect Med; 2014; 4

Park DE, Cheng J, Berrios C, Montero J, Cortés-Cros M, Ferretti S et al. Dual inhibition of MDM2 and MDM4 in virus-positive Merkel cell carcinoma enhances the p53 response. Proc. Natl. Acad. Sci. U. S. A. National Academy of Sciences; 2019; 116:1027–32

Park DE, Cheng J, Mcgrath JP, Lim MY, Cushman C, Swanson SK et al. Merkel Cell polyomavirus activates LSD1-mediated blockade of non-canonical BAF to regulate transformation and tumorigenesis. Nat. Cell Biol. Springer US; 2020; 22:603–6015

Paulson KG, Park SY, Vandeven NA, Lachance K, Thomas H, Chapuis AG et al. Merkel cell carcinoma: Current US incidence and projected increases based on changing demographics. J. Am. Acad. Dermatol. Mosby Inc; 2018; 78:457–463.e2

Perdigoto CN, Bardot ES, Valdes VJ, Santoriello FJ, Ezhkova E. Embryonic maturation of epidermal Merkel cells is controlled by a redundant transcription factor network. Development 2014; 141:4690–6 [PubMed: 25468937]

Peterson SC, Eberl M, Vagnozzi AN, Belkadi A, Veniaminova NA, Verhaegen ME et al. Basal Cell Carcinoma Preferentially Arises from Stem Cells within Hair Follicle and Mechanosensory Niches. Cell Stem Cell. Cell Press; 2015; 16:400–12

Richards KF, Guastafierro A, Shuda M, Toptan T, Moore PS, Chang Y. Merkel cell polyomavirus T antigens promote cell proliferation and inflammatory cytokine gene expression. J. Gen. Virol. Microbiology Society; 2015; 96:3532–44

Rush PS, Rosenbaum JN, Roy M, Baus RM, Bennett DD, Lloyd RV. Insulinoma-associated 1: A novel nuclear marker in Merkel cell carcinoma (cutaneous neuroendocrine carcinoma). J. Cutan. Pathol. Blackwell Publishing Ltd; 2018; 45:129–35

Salic A, Mitchison TJ. A chemical method for fast and sensitive detection of DNA synthesis in vivo. Proc. Natl. Acad. Sci. U. S. A 2008; 105:2415–20 [PubMed: 18272492]

Schneider MR, Schmidt-Ullrich R, Paus R. The Hair Follicle as a Dynamic Miniorgan. Curr. Biol. Cell Press; 2009; 19:R132–42

Sheng W, LaFleur MW, Nguyen TH, Chen S, Chakravarthy A, Conway JR et al. LSD1 Ablation Stimulates Anti-tumor Immunity and Enables Checkpoint Blockade. Cell. Cell Press; 2018; 174:549–563.e19

Shi G, Sohn KC, Li Z, Choi DK, Park YM, Kim JH et al. Expression and Functional Role of Sox9 in Human Epidermal Keratinocytes. PLoS One. Public Library of Science; 2013; 8:e54355

Shuda M, Feng H, Kwun HJ, Rosen ST, Gjoerup O, Moore PS et al. T antigen mutations are a human tumor-specific signature for Merkel cell polyomavirus. Proc. Natl. Acad. Sci. U. S. A. National Academy of Sciences; 2008; 105:16272–7

Shuda M, Guastafierro A, Geng X, Shuda Y, Ostrowski SM, Lukianov S et al. Merkel cell polyomavirus small t antigen induces cancer and embryonic merkel cell proliferation in a transgenic mouse model. PLoS One. Public Library of Science; 2015; 10

Shuda M, Kwun HJ, Feng H, Chang Y, Moore PS. Human Merkel cell polyomavirus small T antigen is an oncoprotein targeting the 4E-BP1 translation regulator. J. Clin. Invest 2011; 121:3623–34 [PubMed: 21841310]

Sihto H, Kukko H, Koljonen V, Sankila R, Böhling T, Joensuu H. Merkel cell polyomavirus infection, large T antigen, retinoblastoma protein and outcome in Merkel cell carcinoma. Clin. Cancer Res 2011; 17:4806–13 [PubMed: 21642382]

Skedung L, El Rawadi C, Arvidsson M, Farcet C, Luengo GS, Breton L et al. Mechanisms of tactile sensory deterioration amongst the elderly. Sci. Reports 2018 81. Nature Publishing Group; 2018; 8:1–10

Spurgeon ME, Cheng J, Bronson RT, Lambert PF, DeCaprio JA. Tumorigenic activity of merkel cell polyomavirus T antigens expressed in the stratified epithelium of mice. Cancer Res 2015; 75:1068–79 [PubMed: 25596282]

Stakaityte G, Wood JJ, Knight LM, Abdul-Sada H, Adzahar NS, Nwogu N et al. Merkel cell polyomavirus: Molecular insights into the most recently discovered human tumour virus. Cancers (Basel). MDPI AG; 2014. p. 1267–97

Sundqvist B, Sihto H, von Willebrand M, Böhling T, Koljonen V. LRIG1 is a positive prognostic marker in Merkel cell carcinoma and Merkel cell carcinoma expresses epithelial stem cell markers. Virchows Arch. Virchows Arch; 2021; 479:1197–207 [PubMed: 34331569]

Sur M, AlArdati H, Ross C, Alowami S. TdT expression in Merkel cell carcinoma: potential diagnostic pitfall with blastic hematological malignancies and expanded immunohistochemical analysis. Mod. Pathol. Mod Pathol; 2007; 20:1113–20 [PubMed: 17885674]

Tang CK, Toker C. Trabecular carcinoma of the skin: Further clinicopathologic and ultrastructural study. Mt. Sinai J. Med 1979; 46:516–23 [PubMed: 317141]

Thibault K Evidence of an epithelial origin of Merkel cell carcinoma. Mod. Pathol. 2021. Nature Publishing Group; 2021; 35:446–8

Tilling T, Moll I. Which Are the Cells of Origin in Merkel Cell Carcinoma? J. Skin Cancer. Hindawi Publishing Corporation; 2012; 2012

Tolstov YL, Pastrana DV, Feng H, Becker JC, Jenkins FJ, Moschos S et al. Human Merkel cell polyomavirus infection II. MCV is a common human infection that can be detected by conformational capsid epitope immunoassays. Int. J. Cancer. John Wiley & Sons, Ltd; 2009; 125:1250–6

Uhlig R, Abboud M, Gorbokon N, Lennartz M, Dwertmann Rico S, Kind S et al. Cytokeratin 10 (CK10) expression in cancer: A tissue microarray study on 11,021 tumors. Ann. Diagn. Pathol. Ann Diagn Pathol; 2022; 60

Verhaegen ME, Harms PW, Van Goor JJ, Arche J, Patrick MT, Wilbert D et al. Direct cellular reprogramming enables development of viral T antigen-driven Merkel cell carcinoma in mice. J. Clin. Invest. American Society for Clinical Investigation; 2022; 132(7)

Verhaegen ME, Mangelberger D, Harms PW, Eberl M, Wilbert DM, Meireles J et al. Merkel cell polyomavirus small T antigen initiates merkel cell carcinoma-like tumor development in mice. Cancer Res 2017; 77:3151–7 [PubMed: 28512245]

Verhaegen ME, Mangelberger D, Harms PW, Vozheiko TD, Weick JW, Wilbert DM et al. Merkel cell polyomavirus small T antigen is oncogenic in transgenic mice. J. Invest. Dermatol. Elsevier Masson SAS; 2015; 135:1415–24

Wang X, Li J, Schowalter RM, Jiao J, Buck CB, You J. Bromodomain protein Brd4 plays a key role in Merkel cell polyomavirus DNA replication. PLoS Pathog. PLoS Pathog; 2012; 8:e1003021 [PubMed: 23144621]

Wollina U, Mahrle G. Epidermal Merkel cells in psoriatic lesions: immunohistochemical investigations on neuroendocrine antigen expression. J. Dermatol. Sci. J Dermatol Sci; 1992; 3:145–50 [PubMed: 1498093]

Woo SH, Lumpkin EA, Patapoutian A. Merkel cells and neurons keep in touch. Trends Cell Biol. Trends Cell Biol; 2015; 25:74–81 [PubMed: 25480024]

Woo SH, Stumpfova M, Jensen UB, Lumpkin EA, Owens DM. Identification of epidermal progenitors for the Merkel cell lineage. Development 2010; 137:3965–71 [PubMed: 21041368]

Wright MC, Logan GJ, Bolock AM, Kubicki AC, Hemphill JA, Sanders TA et al. Merkel cells are long-lived cells whose production is stimulated by skin injury. Dev. Biol. Academic Press; 2017; 422:4–13

Wright MC, Reed-Geaghan EG, Bolock AM, Fujiyama T, Hoshino M, Maricich SM. Unipotent, Atoh1+ progenitors maintain the Merkel cell population in embryonic and adult mice. J. Cell Biol. The Rockefeller University Press; 2015; 208:367

Xiao Y, Thoresen DT, Williams JS, Wang C, Perna J, Petrova R et al. Neural Hedgehog signaling maintains stem cell renewal in the sensory touch dome epithelium. Proc. Natl. Acad. Sci. U. S. A 2015; 112:7195–200 [PubMed: 26015562]

Xu Z, Wang W, Jiang K, Yu Z, Huang H, Wang F et al. Embryonic attenuated Wnt/β-catenin signaling defines niche location and long-term stem cell fate in hair follicle. Elife. eLife Sciences Publications Ltd; 2015; 4:e10567

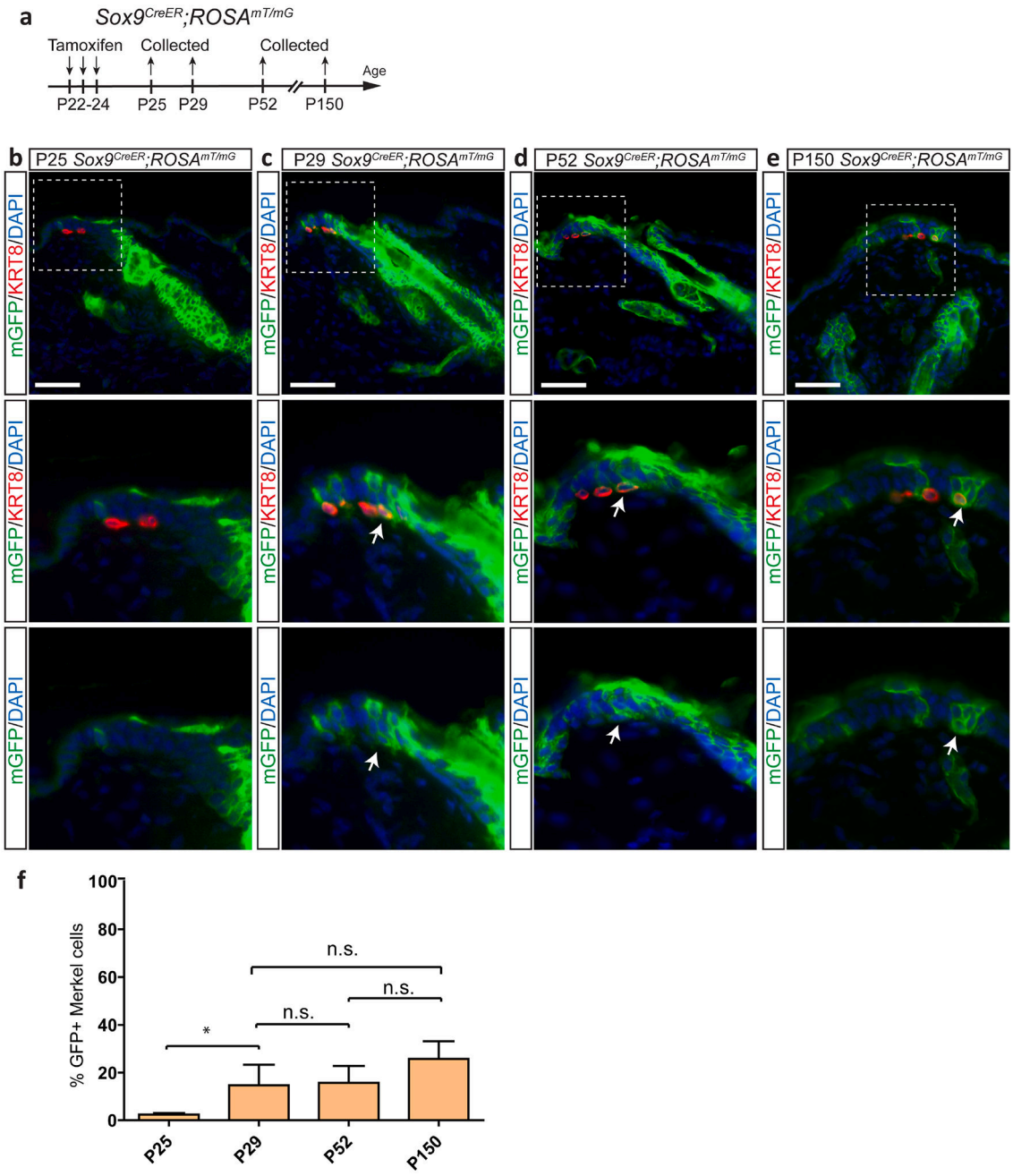

Figure 1: SOX9+ cells are Merkel cell progenitors in postnatal skin.

(a) Experimental design for *Sox9*^{CreER};*ROSA*$^{mT/mG}$ lineage tracing. **(b-e)** *Sox9*^{CreER};*ROSA*$^{mT/mG}$ lineage tracing. Merkel cells marked by KRT8 (red), SOX9+ cells and progeny are labeled by GFP (green). Arrows point to GFP+ Merkel cells at P29 (c), P52 (d), and P150 (e). Note absence of GFP+ KRT8+ cells at P25 and GFP expression in hair follicle. Scale bars=50 μm. **(f)** Quantification of KRT8+ GFP+ Merkel cells in *Sox9*^{CreER};*ROSA*$^{mT/mG}$ back skin. Data are presented as mean percentage of KRT8+ cells co-labeled with GFP. Error bar indicates greatest percentage recorded per time point. Sample

sizes: P25 *n=4*, P29 *n=6*, P52 *n=4*, P150 *n=4*; animals from at least two independent litters.
* p= 0.0079, n.s. not significant (Mann-Whitney test).

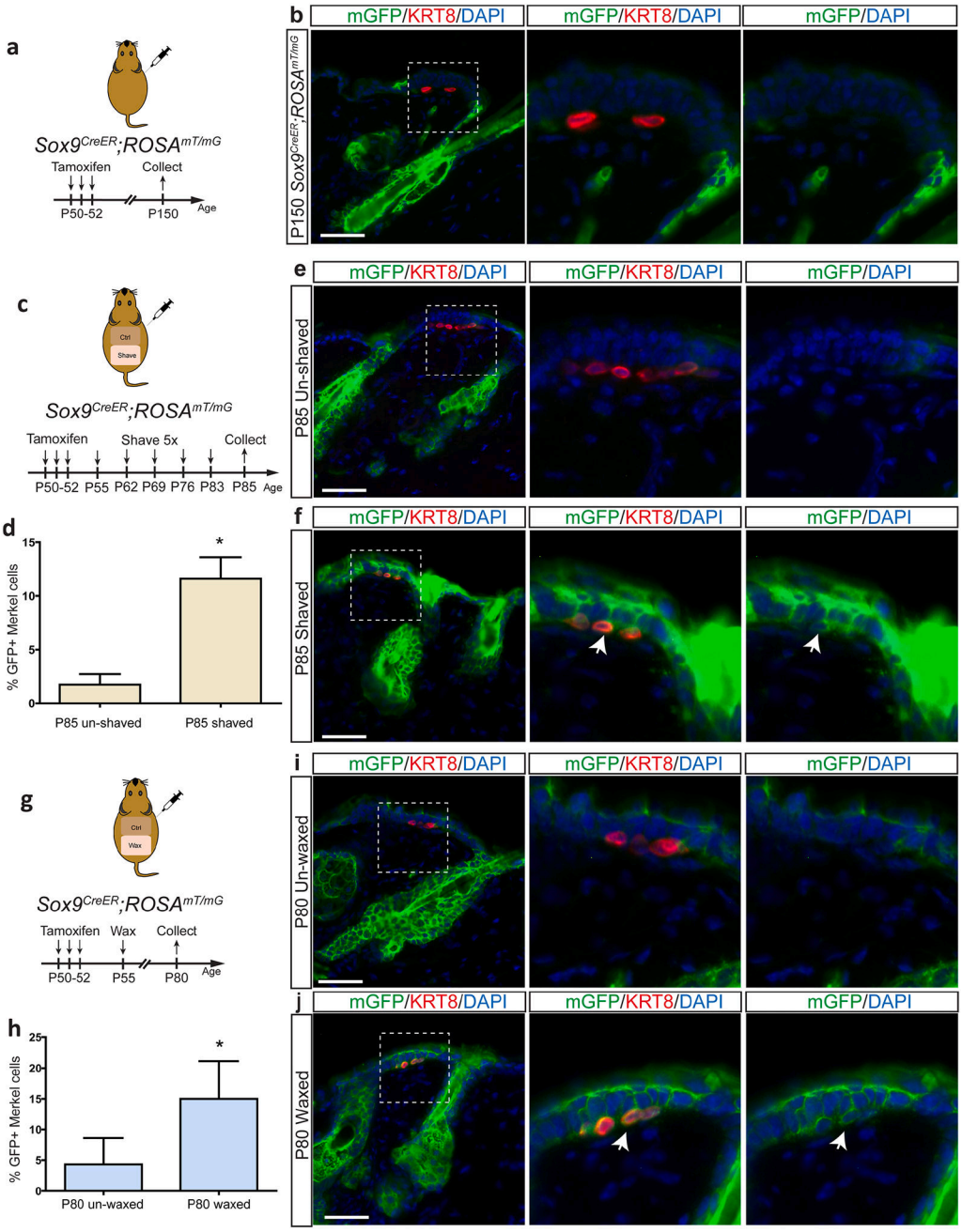

Figure 2: SOX9+ cells retain Merkel cell regeneration potential in adulthood.

(**a**) Design for P50 lineage tracing of SOX9+ progeny in *Sox9*^{CreER};*ROSA*$^{mT/mG}$ mice. (**b**) Lineage tracing at P150. Merkel cells are KRT8+ (red), SOX9+ progeny are GFP+ (green). (**c**) Design for lineage tracing of SOX9+ progeny in shaved skin of *Sox9*^{CreER};*ROSA*$^{mT/mG}$ mice. (**d**) Quantification of GFP+ KRT8+ cells after shaving. *n=3* mice from separate litters. * p= 0.05 (Mann-Whitney). (**e, f**) Lineage tracing in un-shaved (e) or shaved (**f**) skin. Merkel cells are KRT8+ (red), SOX9+ progeny is GFP+ (green). Arrows indicate GFP+ Merkel cells. (**g**) Design for lineage tracing of SOX9+ progeny in waxed skin of *Sox9*^{CreER};*ROSA*$^{mT/mG}$ mice. (**h**) Quantification of GFP+ KRT8+ cells after waxing. *n=3*

mice from separate litters. * p= 0.05 (Mann-Whitney). (**i, j**) Lineage tracing in un-waxed (**i**) or waxed (**j**) skin. Merkel cells are KRT8+ (red), SOX9+ cells and progeny are GFP+ (green). Arrows indicate GFP+ Merkel cells.

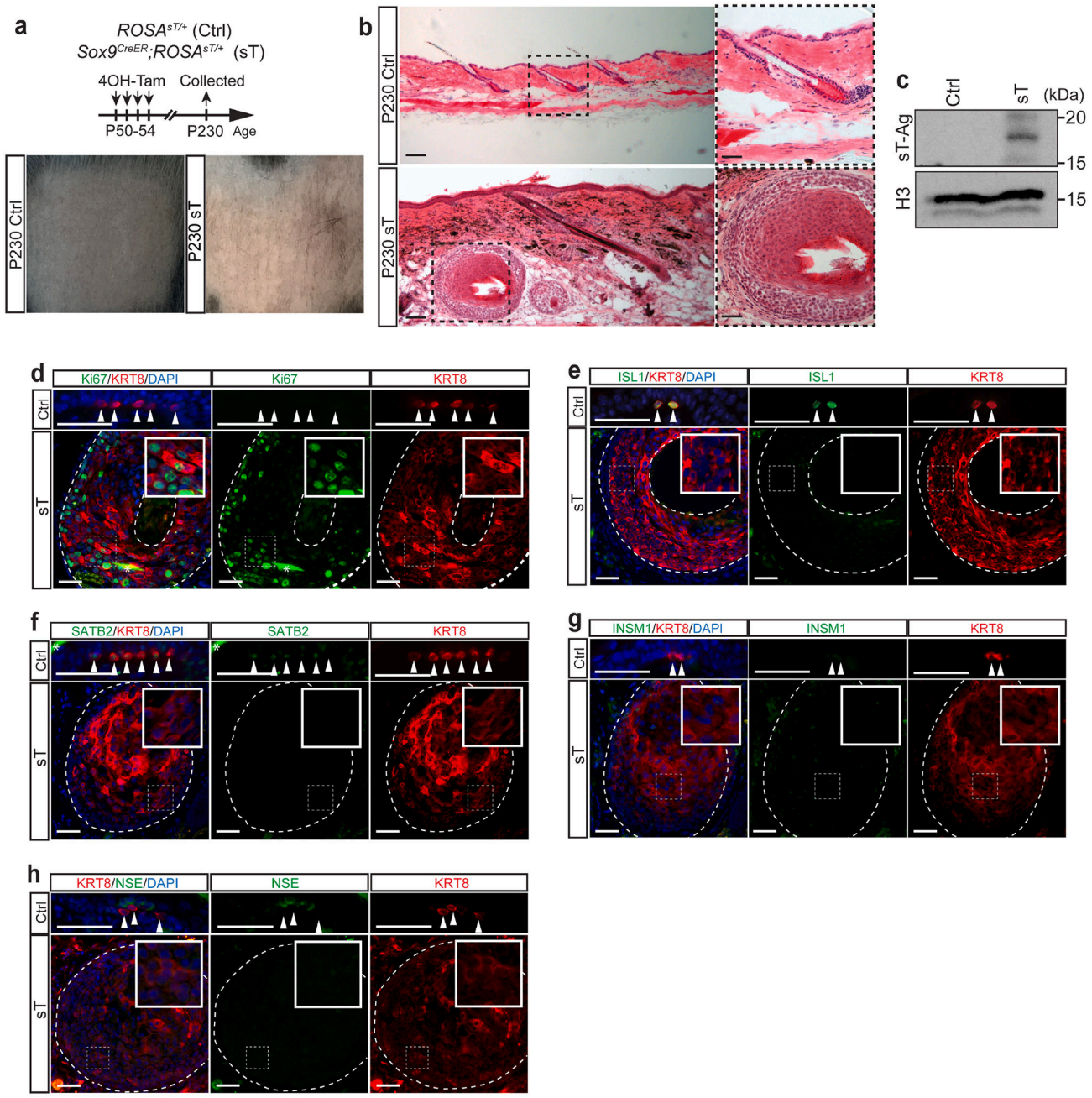

Figure 3: MCV sT-Ag generates cutaneous lesions from SOX9+ cells.

(a) Design for *Sox9*^{CreER};*ROSA*$^{sT/+}$ (sT) mice. Photograph of P230 back skin from sT and control (Ctrl) mice. (**b**) Representative H&E staining of sT lesions and Ctrl skin at 5X (right) and 20X (left) magnification. Scale bars=100 μm (5X), 50 μm (20X). (**c**) Western blot for MCV sT-Ag and Histone 3 (H3) loading control in Ctrl skin and sT lesions. (**d**) IF for proliferation marker Ki67 (green) and KRT8 (red) in sT lesions and control. (**e-h**) Representative images of sT lesions and Ctrl skin co-stained with KRT8 (red) and ISL1 (e, green), SATB2 (f, green), INSM1 (g, green), or NSE (h, green). Arrowheads indicate Merkel cells. Borders of lesions in white. Asterisks indicate autofluorescence. Scale bars=50 μm.

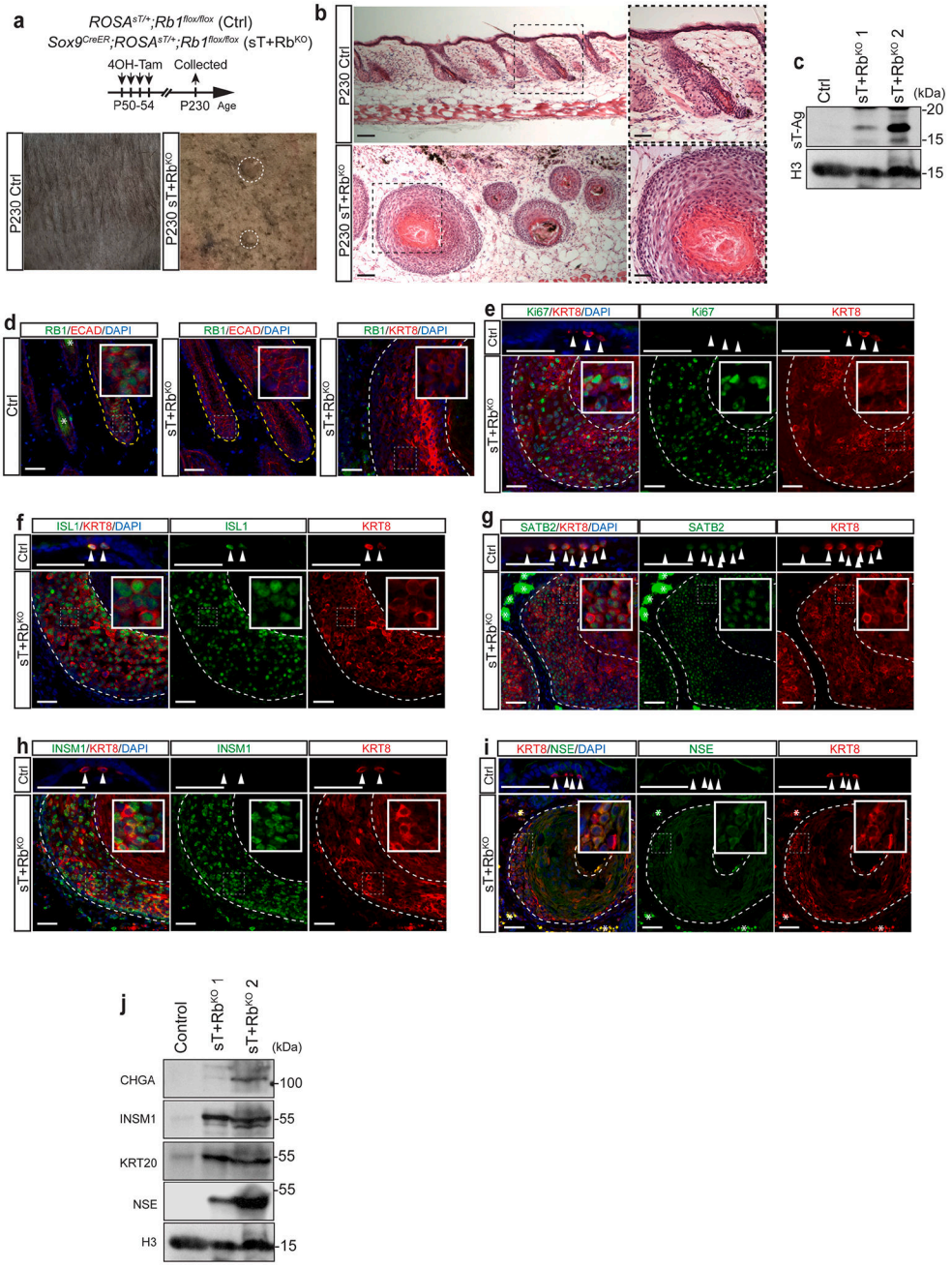

Figure 4: sT-Ag and Rb1 loss promote neuroendocrine reprogramming of SOX9-derived tumors.

(a) Design for *Sox9*^{CreER};*ROSA*$^{sT/+}$;*Rb*$^{flox/flox}$ (sT+Rb^{KO}) mice. P230 skin of control (Ctrl) and sT+Rb^{KO} mice; white circles indicate tumors. **(b)** H&E of sT+Rb^{KO} and Ctrl skin at 5X (right) and 20X (left) magnification. Scale bars=100 μm (5X), 50 μm (20X). **(c)** Western blot for MCV sT-Ag and Histone 3 (H3) loading control. **(d)** IF of RB1 (green) and E-cadherin (ECAD, red) in control (right); RB1 (green) and E-cadherin (E-CAD, red) in sT+Rb^{KO} hair follicles (center); RB1 (green) and KRT8 (red) in sT+Rb^{KO} lesion (left). Hair follicle borders in yellow, lesion borders in white. **(e)** IF of Ki67 (green) and KRT8 (red). Arrowheads indicate Merkel cells. Asterisks mark auto-fluorescence. **(f-h)** sT+Rb^{KO} and

Ctrl co-stained for KRT8 (red) with ISL1 (f, green), SATB2 (g, green), INSM1 (h, green), or NSE (i, green). Scale bars=50 μm. **(i)** Western blot for MCC markers CHGA, INSM1, KRT20, and NSE in Ctrl skin and sT+Rb^{KO} lesions. H3 loading control.

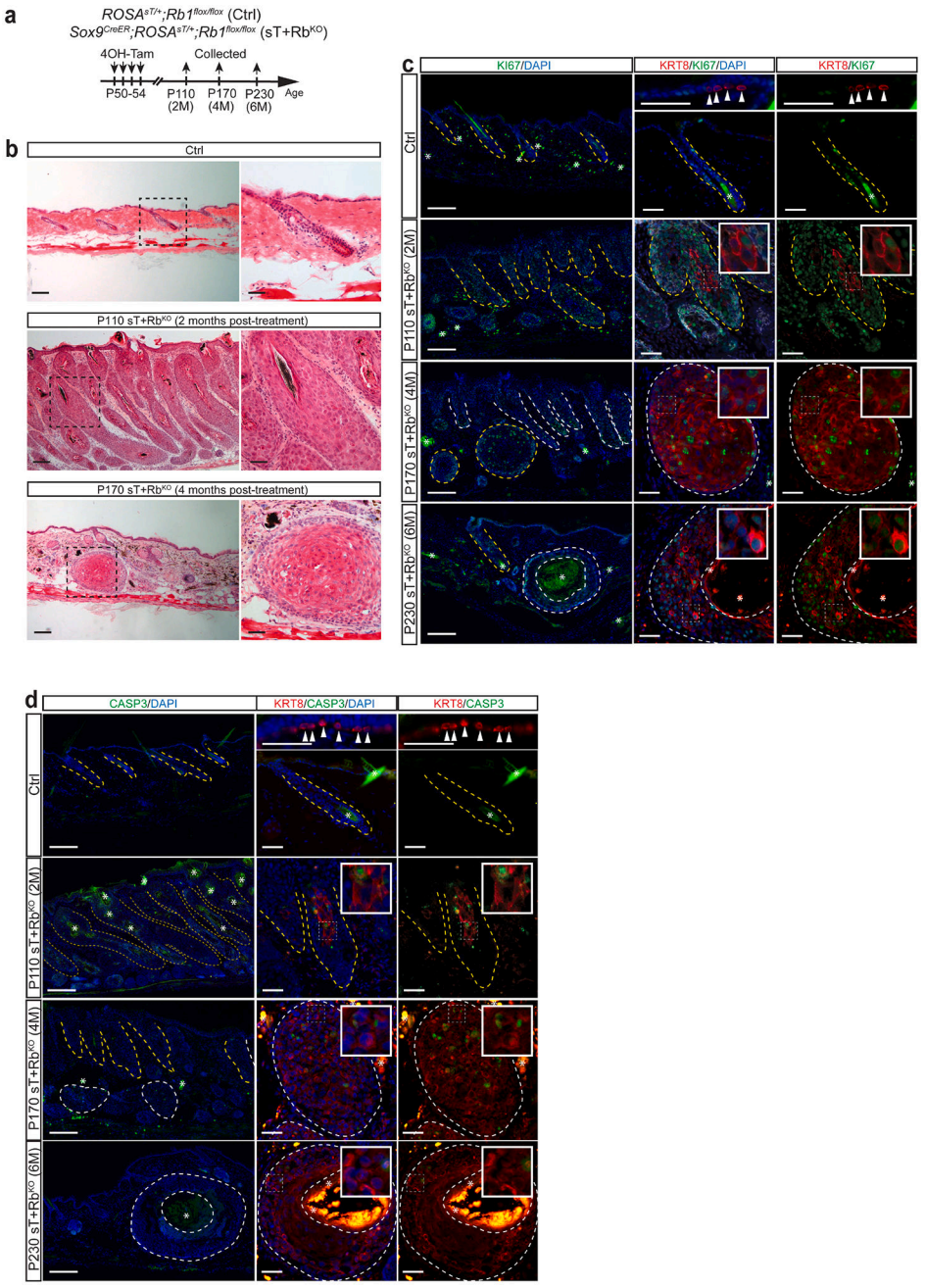

Figure 5: SOX9-derived tumors arise in hair follicles.

(a) Collection scheme for sT+Rb^{KO} mice. **(b)** H&E of control (Ctrl) and sT+Rb^{KO} back skin 2- and 4-months post-treatment. **(c)** IF for Ki67 (green) and KRT8 (red) in Ctrl Merkel cells, Ctrl hair follicles, and sT+Rb^{KO} back skin 2-, 4-, and 6-months post-treatment. 5X magnification (left) and 20X (right). **(d)** IF for activated caspase 3 (CASP3, green) and KRT8 (red) in Ctrl Merkel cells, Ctrl hair follicle, and sT+Rb^{KO} back skin 2-, 4-, and 6-months post-treatment. 5X magnification (left) and 20X (right). Hair follicles outlined in yellow, tumor borders outlined in white. Arrowheads indicate Merkel cells, asterisks mark auto-fluorescence. Scale bars= 200 μm (5X), 50 μm (20X).

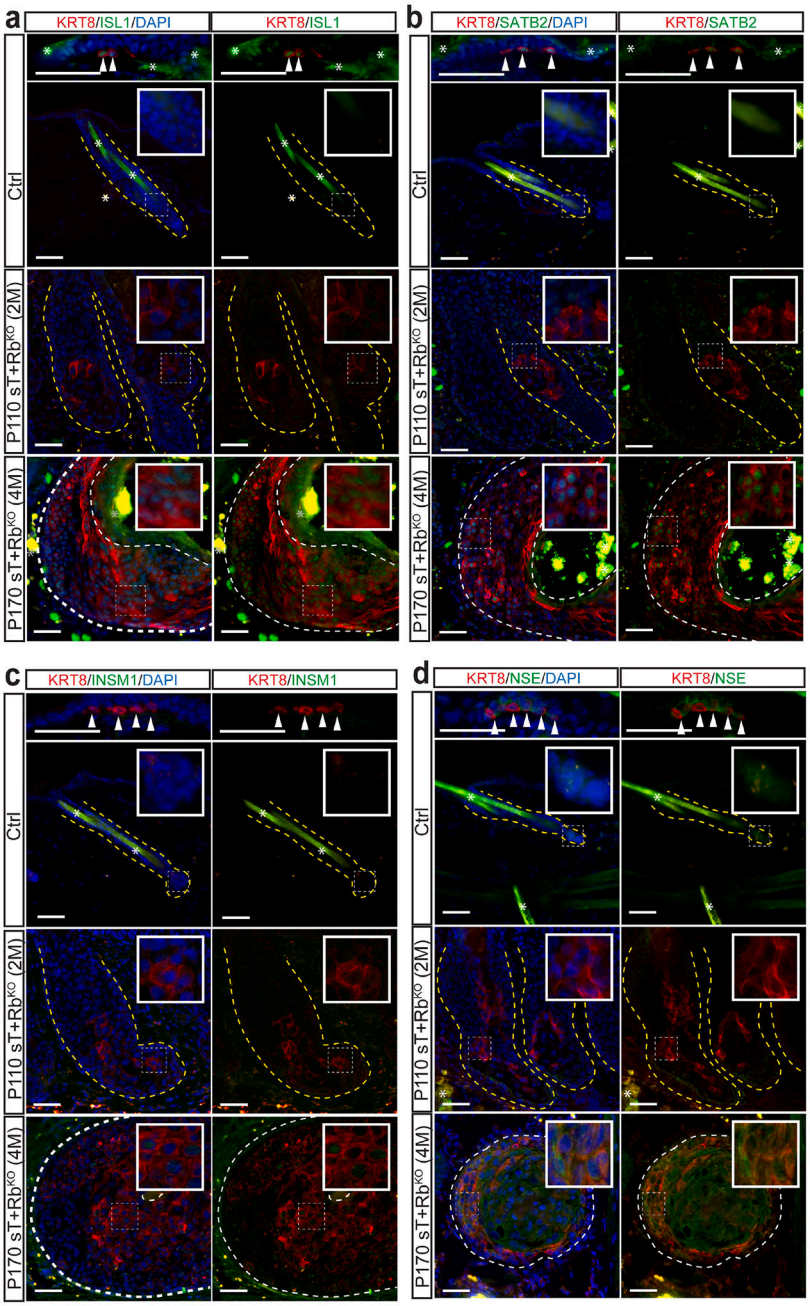

Figure 6: SOX9-derived tumors acquire neuroendocrine marker expression over time.

(a-d) IF in control (Ctrl) Merkel cells, Ctrl hair follicles, and sT+Rb^{KO} lesions 2 months and 4 months post-treatment for KRT8 (red) co-stained with ISL1 (a, green), SATB2 (b, green), INSM1 (c, green), or NSE (d, green). Hair follicle borders are outlined in yellow; lesion borders are outlined in white. Arrowheads indicate Merkel cells, asterisks mark auto-fluorescence. Scale bars=50 μm.

Table 1:

Proportion of cells in sT+RbKO tumors expressing neuroendocrine markers.

	CELLS EXPRESSING MARKER[1]	CELLS CO-POSITIVE WITH KRT8[1]
KRT8	63.19%	100%
KI67	38.52%	41.16%
ISL1	61.71%	45.16%
SATB2	44.88%	34.08%
INSM1	49.76%	33.98%
NSE	58.36%	51.02%

[1]Represented as an averaged proportion of total DAPI-stained nuclei in 10 μm tissue sections from at least 8 unique tumors collected from several different sT+Rb^{KO} mice. KRT8 *n*=50; Ki67 *n*=9; ISL1 *n*=12; SATB2 *n*=8; INSM1 *n*=13; NSE *n*=8.